

EUROFEL-Report-2007-DS5-069

EUROPEAN FEL Design Study



Deliverable N°: D5.6 and D5.7

Deliverable Title: “HOMDYN code upgrade for multibunch beam dynamic simulations” and “Multibunch optimized design of split SC photo-injector”

Subtask : DS-5.2.2

Authors: M. Ferrario , C Vicario and J. Sekutowicz

**Project funded by the European Community
under the “Structuring the European Research Area” Specific Programme
Research Infrastructures action**

INTRODUCTION

A single bunch optimized new working point of a split 1.3 GHz RF superconducting photo-injector for ultra-high brightness beam production has been presented in ref [1]. In the split configuration a short RF gun cavity, typically 1.6 cells long as the one shown in Fig. 1, is followed by a solenoid, located far enough to prevent SC cavity Q degradation, to allow space charge induced emittance growth compensation. The beam is then injected in the linac at well defined energy and spot size in order to fulfill the “invariant envelope” matching conditions for the final damping of emittance oscillations, as discussed in [2].

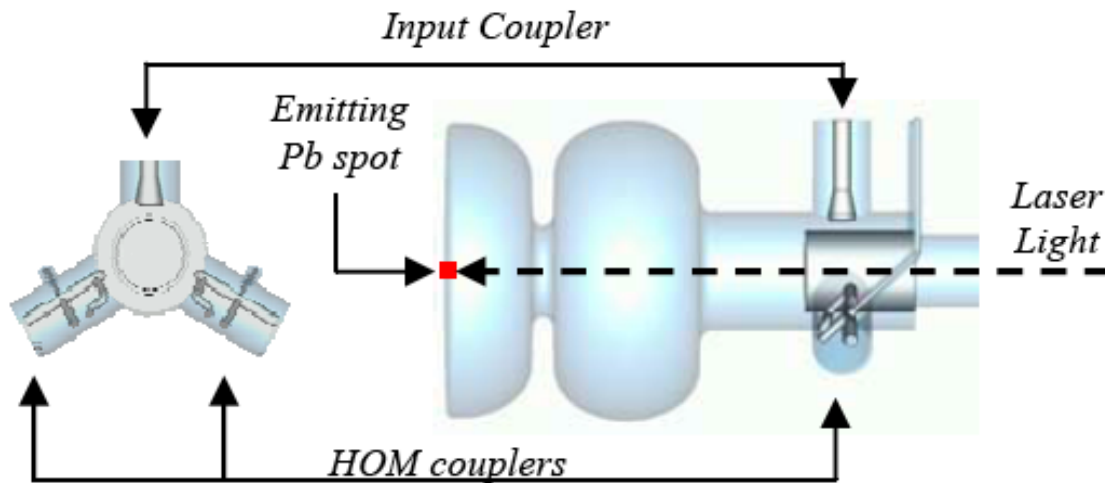


Fig. 1 – Drawing of the 1.6 cells SC RF gun

The first key point of our injector design is the generation of a flat top uniform laser pulse in order to minimize the emittance growth induced by non linear components of space charge fields. A successful experimental demonstration of the possibility to obtain a flat top longitudinal distribution has been obtained by our group [3] during the S-band normal conducting SPARC photoinjector operation [4], showing that a 10 ps long laser pulse can be produced with a TiSa laser system. The scaling to 20 ps as required by our L-band gun design is possible with a modification of the final laser pulse stretcher system.

The second key point of this gun design is the beam matching with the linac. Actually the working point adopted in this design is the same of the SPARC and it is based on the idea of injecting the beam into the linac when a relative emittance maximum occurs and at the same time fulfill the envelope and gradient matching conditions. By doing so the following emittance minimum could be shifted at higher energy and frozen at the lowest value, taking advantage of the additional emittance compensation occurring in the booster. Also this emittance oscillation has been experimentally investigated with the SPARC photoinjector and the results are reported in [4].

Since the main motivation of using a SC RF gun is the possibility to operate in CW or quasi CW regime the bunch to bunch interaction via the voltage induced by the beam itself in the cavity can no longer be neglected. At the beginning of our work no codes were available for multi-bunch simulations of superconducting gun, essentially limited by unaffordable CPU time. For this reason we started to upgrade the fast running code HOMDYN, already used in ref [1] for the single bunch dynamics studies in order to include also the interaction with monopole and dipole Higher Order Modes (HOM) in a superconducting gun. Unfortunately this goal resulted to be too ambitious to be completed during the foreseen time. Nevertheless some progress has been done: we have included in the code the long term beam-cavity

interaction effects limited to the longitudinal monopole modes (TM modes), allowing us to estimate at least the effect of beam loading and multi-bunch energy spread compensation in a RF gun. The single bunch model used in HOMDYN is discussed in ref [5]. In appendix 1 of this paper we report the model upgrade that has been used in this work.

1 BEAM LOADING COMPENSATION TECHNIQUE

The beam loading effect is clearly depicted in Fig. 2 in which an HOMDYN simulation is reported. The beam parameters considered in the computation are the same of **case 1** discussed in the next paragraph. In this case the beam is injected when the cavity voltage has already reached its final steady state, at $t=0$, and no precaution to compensate the beam induced voltage drop has been taken. The final rms relative energy spread along the bunch train for a 1 msec long beam results to be $\sigma_e=6 \times 10^{-2}$, certainly well in excess for our purposes.

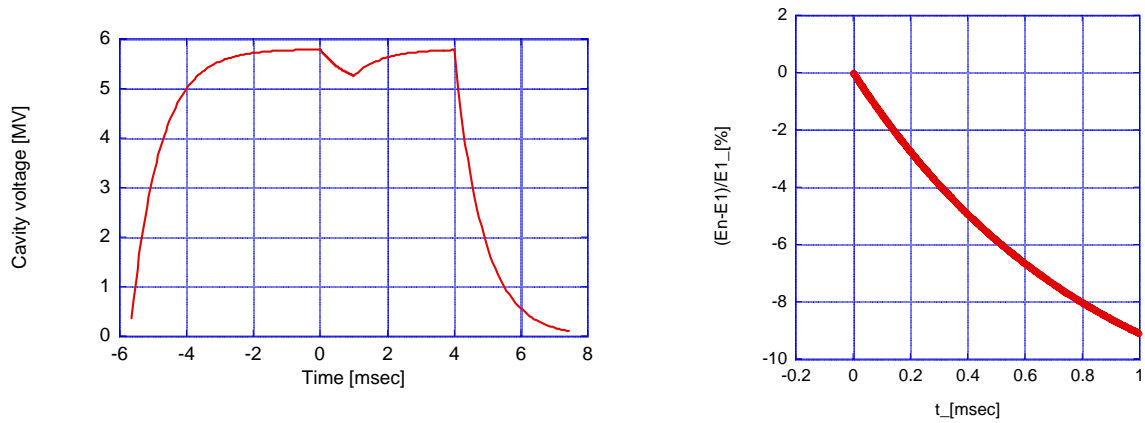


Fig. 2 - Accelerating voltage during the cavity filling and after the beam injection (left plot). Normalized energy gain of a 1 mA beam injected at $t=0$ (right plot). HOMDYN computations.

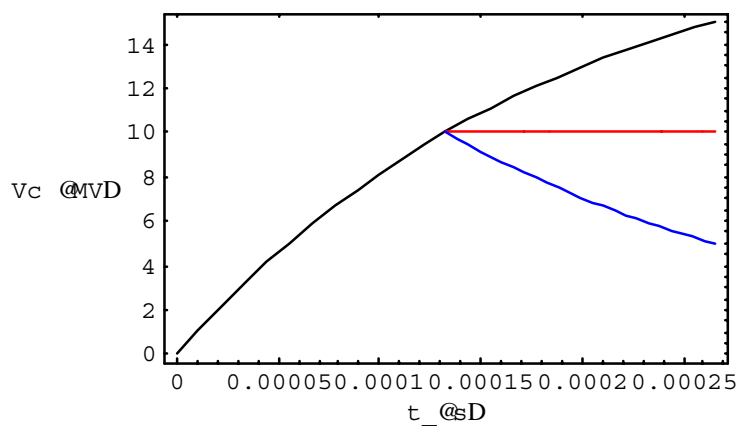


Fig. 3 – The beam induced voltage (blue line) is compensated by the generator voltage (black line) resulting in a constant cavity voltage (red line).

A well know technique for beam loading compensation adopted by the TESLA project [6] and suitable also for a SC gun consists in injecting the beam during the cavity filling so that the beam induced voltage is compensated by the additional voltage provided by the generator, as schematically shown in Fig. 3.

According to the Wilson treatment [7], we can represent the accelerating voltage V_a , the real part of the total cavity voltage V_c , as a superposition of the generator voltage and the beam induced voltage, see also Fig. 4. Including transients the following relation holds for $t \geq t_o$:

$$V_a(t) = V_c(t) \cos \varphi$$

$$= \Re e \left\{ V_{gr} \cos \psi_g e^{i(\psi_g + \vartheta)} \left[1 - e^{-\frac{t}{\tau}(1 - iT_g(\psi_g))} \right] - V_{br} \cos \psi_b e^{i\psi_b} \left[1 - e^{-\frac{(t-t_o)}{\tau}(1 - iT_g(\psi_b))} \right] \right\} \quad (1)$$

where V_{gr} and V_{br} are the steady state generator and beam induced voltages at resonance. The terms between rectangular brackets account for the transient state, t_o being the beam injection time. The angle between the beam current and the cavity voltage is φ , while ϑ is the angle between the beam current and the generator current. The tuning angle is defined as: $\psi = -\text{Arctg}(\Delta\omega\tau)$, where $\Delta\omega = \omega - \omega_\pi$ accounts for an off resonance excitation and $\tau = \frac{2Q_{ext}}{\omega_\pi}$ is the filling time of the fundamental mode resonating at ω_π with a matched external quality factor Q_{ext} .

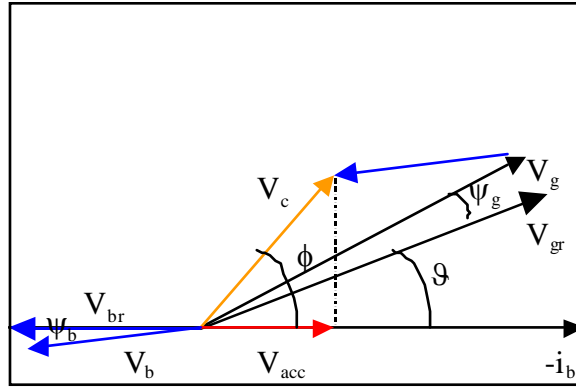


Fig. 4 – Wilson phasor diagram representing generator and beam loading voltage superposition

In the SC RF gun case the beam is injected off crest ($\theta = \phi = \phi_o$), the cavity is excited on resonance ($\psi = 0, \Delta\omega = 0$) and the beam repetition rate is a sub-harmonic of the cavity frequency, so that expression (1) reduces to:

$$V_a(t) = V_{gr} \left[1 - e^{-\frac{t}{\tau}} \right] \cos \phi_o - V_{br} \left[1 - e^{-\frac{(t-t_o)}{\tau}} \right] \quad (2)$$

The optimum beam injection time is the one that results in a constant accelerating voltage, as shown in Fig. 3, and is determined by the following relation:

$$t_o = \tau \ln \left(\frac{V_{gr} \cos \phi_o}{V_{br}} \right) \quad (3)$$

By injecting the beam at the optimum injection time t_o one could expect a perfect compensation of the beam induced voltage, as suggested by Fig. 3. Actually the standard treatment discussed above is not sufficient for a complete analysis of the problem. An additional effect [8] in fact is due to the transient excitation of the lower order modes of the

fundamental pass-band in a multicell structure. Lower order modes contribute differently to the net energy gain from bunch to bunch, due to the fact that each bunch interacts with them with a different relative phase. Moreover in the transient state their voltage could reach a significant fraction of the accelerating mode voltage before decaying, with their damping times, to a very low steady state value.

2 BEAM LOADING COMPENSATION IN A SPLIT SC RF PHOTO-INJECTOR

In a 1.6 cells gun there is only another one mode in the fundamental pass-band to take in to account in addition to the accelerating 1.300 GHz π -mode (with $R/Q = 236$ Ohm),: the 1.286 GHz $\pi/3$ mode (with $R/Q = 43$ Ohm), often improperly called 0-mode [9]. We have found in our design an additional tube mode resonating at 0.866 GHz (with $R/Q = 56$ Ohm) that has to be considered as well since it is strongly coupled with the on axis coaxial power coupler . The form factor of the 3 modes are shown in the following figures.

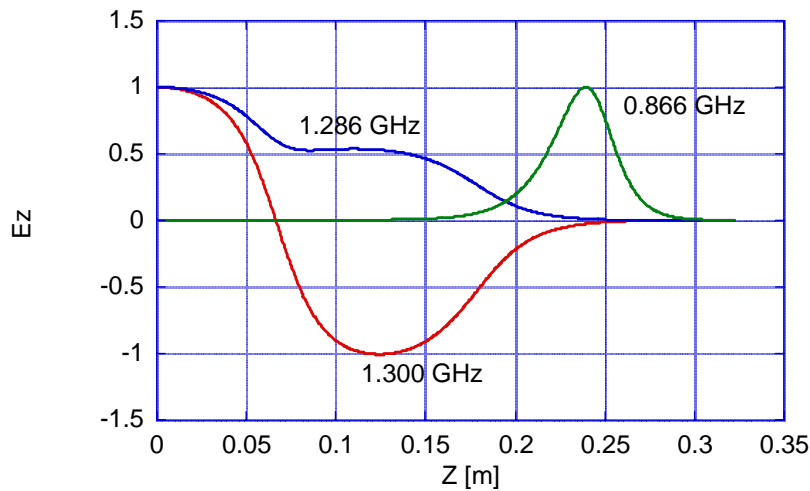


Fig. 5 – Normalized field form factors of the TM_{010} fundamental pass-band and beam tube modes.

With the adjustable length input coupler designed for our RF gun, we can match the generator voltage to the beam current with a Q_{ext} in the range of $10^6 - 10^7$. Assuming a 1 mA design beam current, corresponding to a 1 MHz beam repetition rate each bunch with 1 nC charge, the beam induced voltage range within 0.826 MV (**case 1**, with $Q_{ext} = 3.5 \times 10^6$, $\tau = 0.857$ msec) and 8.26 MV (**case 2**, with $Q_{ext} = 3.5 \times 10^7$, $\tau = 8.57$ msec). We report hereafter the beam loading simulation results for both cases.

In **case 1** according to (3) with $\phi_o = 30^\circ$ the expected injection time suitable for beam loading compensation is $t_o = 1.66$ msec. Figure 6 shows the accelerating voltage during the cavity filling and after the beam injection as computed by HOMDYN. Figure 7 shows instead the cavity stored energy for each mode.

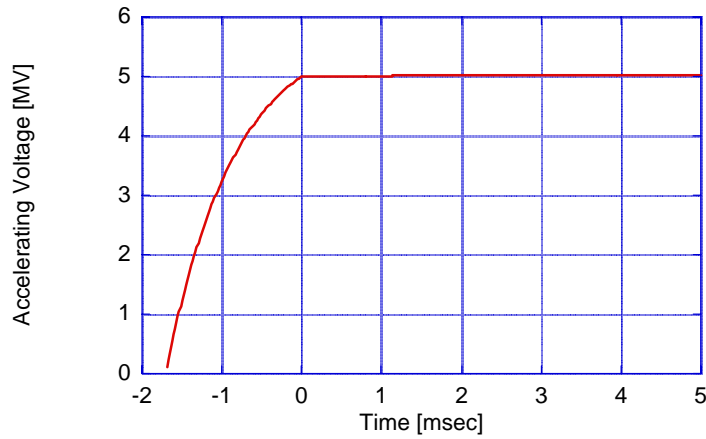


Fig. 6 Accelerating voltage during the cavity filling and after the beam injection.

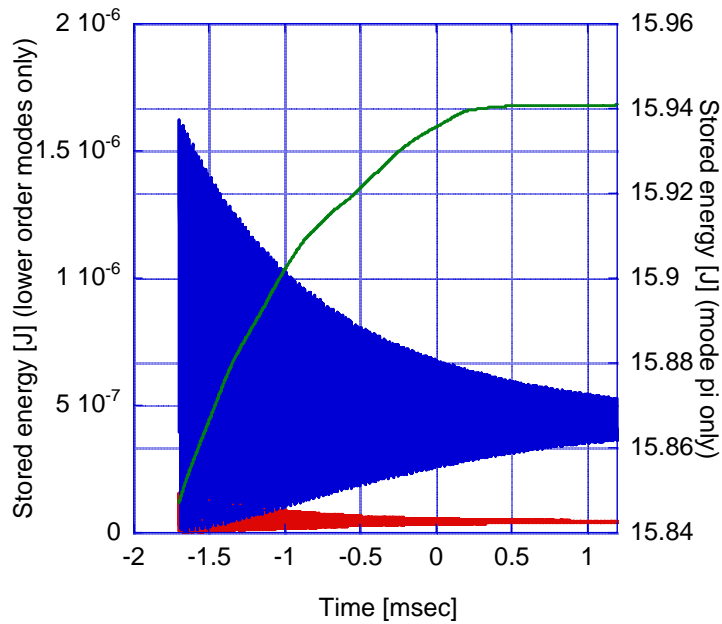


Fig. 7 Stored energy during the cavity filling and after the beam injection. Accelerating mode (green line), $\pi/3$ mode (red line), beam tube mode (blue line).

In Figure 8 is shown the energy gain along the first 1 msec of a 1 mA beam as computed by HOMDYN. As one can see the energy spread compensation along the beam is not fully achieved when one includes in the computation the interaction with all the modes of the accelerating pass-band and the beam tube mode. The relative train energy spread is nevertheless quite small: $\sigma_e=2 \times 10^{-4}$, well within the design specification. Moreover the effect of the lower order modes decay after a few cavity time constant, not clearly visible in the figure since the integration time is too short. Notice that the relative train energy spread reduces to $\sigma_e=1.4 \times 10^{-4}$ if we neglect the interaction with the tube mode (0.866 GHz), as shown in fig. 9.

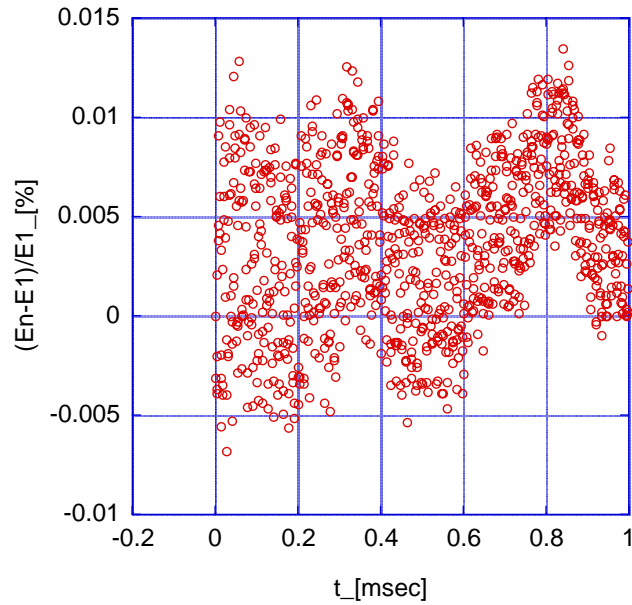


Fig. 8 – Normalized energy gain of a 1 mA beam injected at $t_0=1.7$ msec, as computed by HOMDYN, (the relative train energy spread is $\sigma_e=2 \times 10^{-4}$). Only the first 1000 bunches are shown. The energy gain is normalized to energy gained by the first injected bunch.

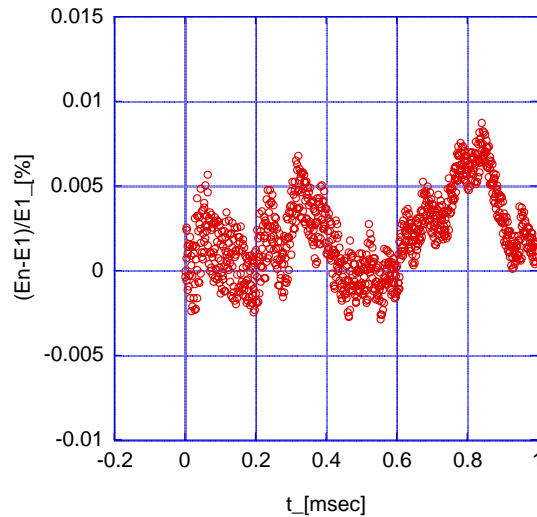


Fig. 9 – The same case of fig. 8 excluding the interaction with the beam tube mode (0.866 GHz). The relative train energy spread is reduced to $\sigma_e=1.4 \times 10^{-4}$.

In **case 2** the expected injection time suitable for beam loading compensation is longer $t_0 = 4.5$ msec. Also in this case we observe an energy spread along the beam with $\sigma_e=2.8 \times 10^{-4}$, as shown in fig. 10, still acceptable for our purposes.

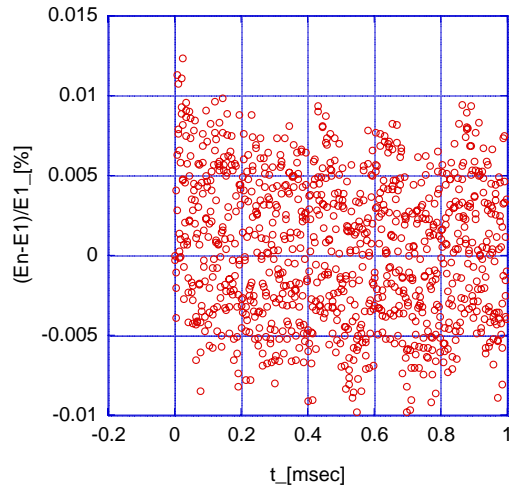


Fig. 10 – Normalized energy gain of a 1 mA beam for the case 2.

3 CONCLUSIONS

Several problems has been found during the HOMDYN code development for the specific application discussed in this report. The main one has been the modeling of beam interaction with dipole modes that requires a wide extension of the code allowing for transverse beam displacement and representation of the coupling current term. As reported in the introduction we didn't succeeded to complete this development and we have used more standard techniques to evaluate the required Q_{ext} for a convenient dumping of the most dangerous HOM, see Tab. 1.

Tab. 1 – HOM of the 1.6 cells RF gun

Mode	f [MHz]	(R/Q)
Dipole: TE111-1a	1641.8	1.85 [Ω/cm^2]
Dipole: TE111-1b	1644.9	1.30 [Ω/cm^2]
Dipole: TM110-1a	1883.5	10.1 [Ω/cm^2]
Dipole: TM110-1b	1884.0	9.99 [Ω/cm^2]
Dipole: TM110-2a	1957.0	3.90 [Ω/cm^2]
Dipole: TM110-2b	1957.1	3.85 [Ω/cm^2]
Monopole: TM011	2176.5	43.2 [Ω]

In addition despite the present version of the code preserve its fast running characteristic, the allocated memory available in our processor is not sufficient for a long beam evolution study. For this reason the case shown in this report has been limited to the first 1 msec of the bunch train propagation inside the cavity.

Nevertheless we can conclude that at least concerning beam loading compensation no significant problem are expected in our RF gun design. In addition we are confident that no

dangerous effect we have to expect from dipole modes interaction, since have adopted the HOM couplers developed for the TESLA cavities [6] which were designed by one of us (Sekutowicz) for a much more severe 8 m A beam.

4 REFERENCES

- [1] M. Ferrario et al., EUROFEL-Report-2005-DS5-009
- [2] L. Serafini, J. B. Rosenzweig, Phys. Rev. E 55 (1997) 7565.
- [3] C. Vicario, et al., Optics Letters 31, 2885 (2006).
- [4] M. Ferrario et al., Phys. Rev. Lett. 99, 234801 (2007)
- [5] M. Ferrario et al., SLAC-PUB-8400.
- [6] “TESLA Technical Design Report”, TESLA Report 2001-23
- [7] P. B. Wilson, “High energy electron linacs: applications to storage ring RF systems and linear colliders”, SLAC-PUB-2884
- [8] J. Sekutowicz, “Transient state in standing wave accelerator structures”, Particle Accelerators, 1994, Vol. 45 (p. 47).
- [9] M. Ferrario and C. Ronsivalle, “Resonant modes in a 1.6 cells RF gun”, Int. J. of Modern Physics A, Vol. 22, No. 23, (2007) 4204-4213

5 APPENDIX 1 - THE HOMDYN MODEL

The HOMDYN code relies on a simple self-consistent model that couples a current density description of beam evolution with the Maxwell equations in the normal modes expansion form. It takes into account single bunch space charge effects, beam loading of a long train of bunches, build-up effects of higher order modes and an on axis localized generator in order to describe the cavity re-filling from bunch to bunch passage. The new code version, still under development, will be suitable for space charge dominated non relativistic beam dynamics computations, especially when transient fields excitation plays an important role as in SC RF gun.

We recall in this appendix the main equations of the model concerning the case under study, with some new features we added recently.

We represent the electric field in the cavity as a sum of normal orthogonal modes:

$$\mathbf{E}(t, \mathbf{r}) = \sum_n \Re e [A_n(t) \mathbf{e}_n(\mathbf{r})] \quad (\text{A1})$$

with complex amplitude

$$A_n(t) = \alpha_n(t) e^{i\omega_n t} = \frac{a_n(t)}{2} e^{i(\omega_n t + \varphi_n(t))} \quad (\text{A2})$$

where $a_n(t)$ is a real amplitude. The field form factors $\mathbf{e}_n(\mathbf{r})$ are any normalized solution of the Helmholtz equation, satisfying the boundary condition $\hat{\mathbf{n}} \times \mathbf{e}_n = 0$ on the cavity surface and the solenoidal condition $\nabla \cdot \mathbf{e}_n = 0$ within the cavity volume. They can be computed by standard finite differences codes like SUPERFISH. In the following we will restrict our attention to the on axis longitudinal electric field components of TM modes.

The modes amplitude equations are:

$$\dot{\tilde{X}}_n + \frac{\omega_n}{Q_n} \tilde{X}_n + \omega_n^2 A_n = -\frac{I}{\varepsilon_o} \frac{d}{dt} \left[\int_V J(z, t) \cdot e_n^*(z) dv \right] \quad (\text{A3})$$

where as a driving current densities we consider the superposition of two terms $\mathbf{J} = \mathbf{J}_g + \mathbf{J}_b$. The term \mathbf{J}_g is a feeding sinusoidal current density, representing a point like power supply on the cavity axis located at z_g . The second term \mathbf{J}_b represents the beam current density. The loaded quality factor Q accounts for the cavity losses.

We have also included the possibility to change the rf pulse rising time τ_g , representing the power supply term as follows:

$$J_g(t, z_g) = \frac{J_g^o}{2i} \delta(z - z_g) \left(1 - e^{-\frac{t}{\tau_g}} \right) e^{i(\omega_l t + \psi_l)} \quad (\text{A4})$$

where J_g^o is the generator strength, ω_l and ψ_l are the generator frequency and phase respectively.

The basic assumption in the description of the beam term consists in representing each bunch as a uniform charged cylinder, whose length L and radius R can vary under a self-similar evolution, i.e. keeping anyway uniform the charge distribution inside the bunch. Further details are reported in [4], we recall here that the beam current density term \mathbf{J}_b can be written for each bunch as follows:

$$J_b(t, z) = \frac{q\beta_{bar}c}{L} [\eta(z - z_t) - \eta(z - z_h)] \quad (\text{A5})$$

where q is the bunch charge, $\beta = v(t)/c$, η is a step function and the indexes h, t refer to bunch head and tail positions respectively. The equations for the longitudinal motion of the bunch barycenter are simply:

$$\dot{\tilde{X}}_{bar} = \beta_{bar}c \quad \dot{\beta}_{bar} = \frac{e}{m_o c \gamma_{bar}^3} E_z(t, z_{bar}) \quad (\text{A6})$$

Substituting the definition (A2) in the modes amplitude equations (A3), under the slowly varying envelope (SVEA) approximation $\frac{d\alpha_n}{dt} \ll \omega_n \alpha_n$ we can neglect the second order derivatives $\frac{d^2 \alpha_n}{dt^2} \ll \omega_n^2 \alpha_n$, and we obtain a first order amplitude equation for each mode:

$$\dot{\tilde{\alpha}}_n + \frac{\omega_n}{2Q_n} \left(1 + \frac{i}{2Q_n} \right) \alpha_n = -\frac{I}{2\omega_n \varepsilon_o} \left(1 + \frac{i}{2Q_n} \right) \frac{d}{dt} \left[\int J(z, t) \cdot e_n^*(z) dz \right] e^{-i\omega_n t} \quad (\text{A7})$$

The SVEA approximation supposes small field perturbations produced by any single bunch, that add up to give an envelope of any field mode slowly varying on the time scale of its period T . Because the characteristic cavity reaction time is of the order of $\tau = \frac{2Q}{\omega} \gg T$ we fulfill the SVEA hypothesis. This approximation allows to reduce the numerical and analytical computing time.

The evolution of the field amplitude during the bunch to bunch interval is given by an analytical solution of equation (A7) with $J_b=0$, which connects successive numerical integration applied during any bunch transit. Taking into account the generator feeding current (A4), with a general initial condition $\alpha_n(t_o)=\alpha_n^o$, the analytical solution of (A7) is:

$$\alpha_n(t) = K_n \left\{ \begin{aligned} & \frac{i\omega_l}{i\Omega_n + \frac{\omega_n}{2Q_n} \left(1 + \frac{i}{2Q_n}\right)} \left[e^{-\left(i\Omega_n + \frac{\omega_n}{2Q_n} \left(1 + \frac{i}{2Q_n}\right)\right)(t-t_o)} - 1 \right] e^{i\Omega_n t} + \\ & + \frac{g - i\omega_l}{i\Omega_n + \frac{\omega_n}{2Q_n} \left(1 + \frac{i}{2Q_n}\right) - g} \left[e^{-\left(i\Omega_n + \frac{\omega_n}{2Q_n} \left(1 + \frac{i}{2Q_n}\right) - g\right)(t-t_o)} - 1 \right] e^{(i\Omega_n - g)t} \end{aligned} \right\} + \alpha_n^o e^{-\frac{\omega_n}{2Q_n} \left(1 + \frac{i}{2Q_n}\right)(t-t_o)} \quad (\text{A8})$$

where $\Omega_n = \omega_l - \omega_n$, $g = \frac{I}{\tau_g}$, and $K_n = \frac{I}{4i\varepsilon_o\omega_n} \left(1 + \frac{i}{2Q_n}\right) J_g^o e^{i\psi_l} e_n(z_g)$.

ANNEX to

D5.6/5.7

STATUS OF Nb-Pb SUPERCONDUCTING RF-GUN CAVITIES

J. Sekutowicz, J. Iversen, D. Klinke, D. Kostin, W. Möller, A. Muhs, DESY, Hamburg, Germany
 P. Kneisel, TJNAF, Newport News, USA
 J. Smedley, T. Rao, BNL, Upton, USA
 P. Strzyżewski, A. Soltan INS, Swierk/Otwock, Poland
 Z. Li, K. Ko, L. Xiao, SLAC, Menlo Park, USA
 R. Lefferts, A. Lipski, SUNY, Stony Brook, USA
 M. Ferrario, INFN, Frascati, Italy

Abstract

We report on the progress and status of an electron RF-gun* made of two superconductors: niobium and lead [1]. The presented design combines the advantages of the RF performance of bulk niobium superconducting cavities and the reasonably high quantum efficiency of lead. The design of RF-gun and performance of 3 test cavities without and with the emitting lead spot are reported in this contribution. Measured quantum efficiency for lead at 2K is presented briefly. More details are reported in [9].

INTRODUCTION

Motivation

Improvement in RF performance of superconducting (sc) cavities over the past decade has made feasible continuous wave (cw) and near-cw operations of superconducting electron linacs at high accelerating gradients. Both operation modes require injectors operating at cw or near-cw, providing low emittance electron beams. An example of such an injector (so called split injector) is discussed in [2]. The most demanding component of a cw injector is the RF-gun, operating in a cw mode and delivering highly populated (~1 nC) low emittance bunches. When generating highly populated low emittance bunches, both room temperature and superconducting RF-guns have to be operated at high accelerating gradients to suppress space charge effects that dilute the emittance. Normal conducting RF-guns face difficulties in meeting this requirement in the cw or near-cw mode. Their copper walls dissipate many kilowatts of power in fulfilling high gradient conditions even when they operate at low pulse repetition rate. Superconducting RF-guns (SRF-guns) dissipate orders of magnitude less power than the normal conducting devices. They can be operated at high duty factor. The challenge here is integration of a non superconducting photo-cathode into a sc cavity [3] in a way that preserves its original high intrinsic quality factor Q_0 (small cryogenic losses). One possible solution to this problem, based on a choke filter design, is investigated at Forschungszentrum Rossendorf [4, 5]. Another approach, very attractive and technically feasible for miliampere-class SRF-guns, is to use a superconducting material as

the photo-cathode. In this case, difficulties arise from the moderate quantum efficiency (QE) of the superconducting materials, which must be compensated with shorter wave-length and higher pulse energy of the illuminating laser. The niobium cathode proposed and tested at BNL [6] demonstrates rather poor QE . A complementary approach with lead [7] is discussed in the following section.

LEAD QE AND RF-DESIGN

QE of Lead

Lead has superior QE to niobium. Test results of lead QE at room temperature were reported by us in [8]. Fig. 1 shows the summary of the tests at 300 K vs. photon energy E_p for niobium, bulk lead and lead samples deposited with various techniques. The highest QE of 0.55% has been measured for the arc-deposited sample illuminated with 6.5 eV photons. For 5.8 eV photons (5th harmonics of 1064 nm infrared laser) the QE of that sample was still 0.25%. QE of the electroplated and magnetron deposited samples at this photon energy is ~0.17%. Generation of 1 nC bunch with this QE will require 3.4 μ J energy per pulse on the cathode. The cold QE test was done very recently and is reported elsewhere in these proceedings [9].

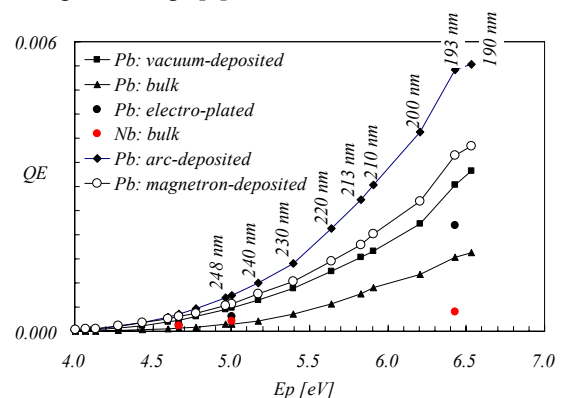


Figure 1: Measured QE of lead deposited with various coating methods. Bulk Pb and Nb data are displayed for comparison.

RF-Design

In the hybrid Pb-Nb gun, a small emitting spot of lead ($\varnothing < 3$ mm) will be located in the center of the back wall of

* This work has been partially supported by the EU Commission, contract no. 011935 EUROFEL-DS5 and US DOE under contract number DE-AC02-98CH10886.

the 0.6-cell of a 1.6-cell[†] cavity (Fig. 2), which will be made of high purity niobium. The cavity, equipped with two HOM couplers, input coupler and pickup probe will be assembled for operation in a dedicated cryostat. The gun is designed to be implemented in the split injector. A solenoid, installed directly after the cavity, will be used for emittance growth compensation. Tables 1 and 2 and Figure 3 show RF-parameters and the Higher Order Mode (HOM) suppression (Q_{ext}) for the present design. The damping of HOMs in a SRF-gun is crucial for the beam quality, which can be diluted by the interaction between non-relativistic electrons (in the first 0.6-cell) with deflecting dipole modes. The operating electric field on the lead cathode E_{peak} will not exceed 60 MV/m. At this field, the emitting spot will be exposed to $B = 4$ mT, which is much smaller than the lead critical magnetic flux $B_c = 70$ mT.

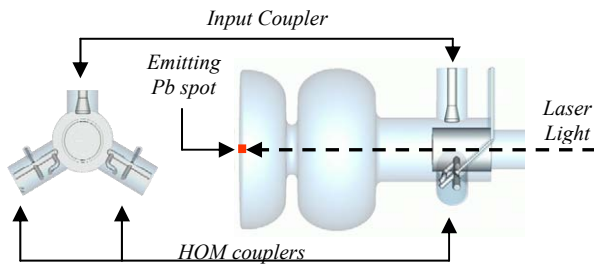


Figure 2: 1.6-cell SRF-gun cavity with 2 HOM couplers and the input coupler.

Table 1: RF-parameters of the 1.6-cell SRF gun

Parameter	Unit	Value
π -mode frequency	[MHz]	1300
0-mode frequency	[MHz]	1286.5
Cell-to-cell coupling	-	0.015
Active length $1.6 \cdot \lambda/2$	[m]	0.185
Nominal E_{cath} at cathode	[MV/m]	60
Energy stored at nominal E_{cath}	[J]	20
Nominal beam energy	[MeV]	6

Table 2: HOMs of 1.6-cells

Mode	f [MHz]	(R/Q)
Dipole: TE111-1a	1641.8	1.85 [Ω/cm^2]
Dipole: TE111-1b	1644.9	1.30 [Ω/cm^2]
Dipole: TM110-1a	1883.5	10.1 [Ω/cm^2]
Dipole: TM110-1b	1884.0	9.99 [Ω/cm^2]
Dipole: TM110-2a	1957.0	3.90 [Ω/cm^2]
Dipole: TM110-2b	1957.1	3.85 [Ω/cm^2]
Monopole: TM011	2176.5	43.2 [Ω]

Two types of half-cell resonators have been built to measure the QE of lead at 2 K and to test the RF performance of Nb-Pb cavities. Both types are shown in

[†] The first cell is $0.6 \cdot \lambda/2$ long. This length provides the lowest emittance growth.

Fig. 4. The left one was built at TJNAF. It has an opening in the center of the back wall, which is vacuum sealed with a niobium plug and an indium gasket. The advantage of this cavity type is that plugs can be easily coated with emitting materials to test various deposition methods and various superconductors for photoemission.

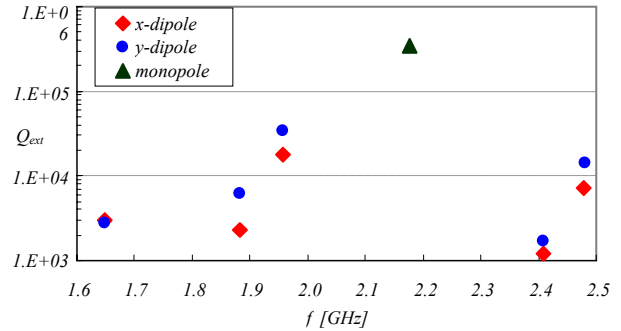


Figure 3: 3D modelling of the HOM suppression for the 1.6-cell SRF-gun.

It can be an alternative solution to the second cavity type, built at DESY (Fig. 4, right), in which, the technically difficult coating is done directly on the back wall. An additional difficulty in this version is that the emitting spot must withstand cleaning procedures applied to the cavity. Two of the cleaning steps could degrade QE : chemical treatment and high pressure water rinsing. Both procedures are essential for good performance of sc cavities. On the other hand, two features make this version very attractive: the smooth back wall does not enhance locally the electric field near the cathode and there is no RF electric contact needed in the high field region, which may reduce the intrinsic Q_o of the cavity. The plug cavity and the first DESY cavity were tested several times without and with lead coating. The baseline test without the coating, of the second DESY cavity fabricated in 2006, was recently carried out at TJNAF.

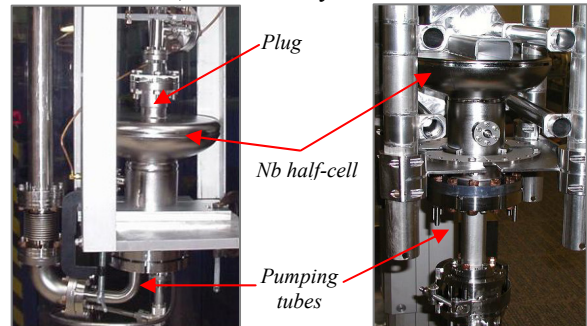


Figure 4: Test half-cell cavities built at TJNAF (left) and at DESY (right) assembled on inserts for the RF-cold test.

RF-PERFORMANCE TEST

Cold Test without Coating

Figure 5 displays the best results for the half-cell cavities without lead coating on the back wall and on the plug. The tests showed that chemical treatment and high pressure water rinsing are challenging for the half-cells and need to be improved in the future. We observed,

testing DESY type cavities, few multipacting levels between 30 and 40 MV/m, which could be processed for cavities without lead. It took some time to overcome these levels by RF-processing. In the plug cavity, we observed heating of the first plug version, which was due to insufficient cooling by LHe. The cooling was improved for the tests shown.

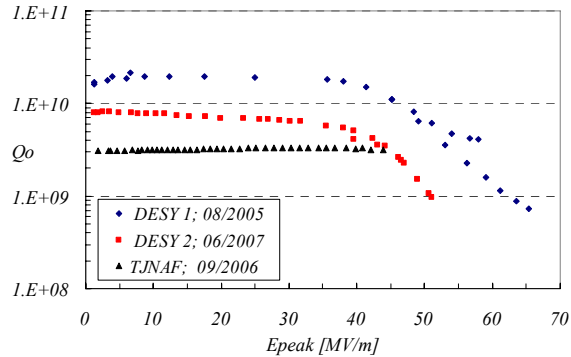


Figure 5: Cold (2K) RF-test results without lead coating.

Cold Test with Lead Coating

The emitting 4 mm diameter lead spot at the center of the back wall of the DESY cavity was deposited by the arc-discharge method at A. Soltan INS. The 7 mm diameter plug of the TJNAF cavity was electroplated with lead at Stony Brook University. As mentioned before, the final cleaning of the cavities is challenging, especially for the DESY type when coated. That cavity reached 40 MV/m peak field (Fig. 6), but a lot of processing events and heavy radiation was observed during the cold test. The second DESY cavity will be coated and tested soon. The TJNAF cavity is somewhat easier to clean because of the absence of the coated plug during surface treatment. It demonstrated almost the same performance as without lead, which confirms our expectation that the emitting spot located on axis should not limit the performance.

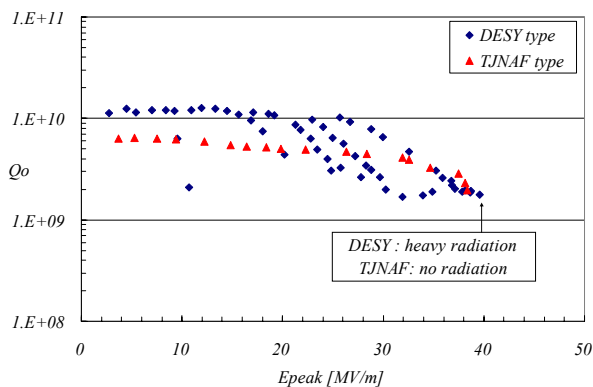


Figure 6: Cold (2K) RF-test results with lead coating.

Irradiation with Laser

One of our concerns from the very beginning of this project was the recombination time of broken Cooper pairs in the emitting spot by the irradiating laser. The theoretical investigation presented in [1] led to the conclusion that the recombination time strongly depends

on temperature. Fortunately, the time is shorter for higher temperature. The 248 nm excimer laser used for the cold tests generated 5.3 ns long pulses (FWHM) at up to 250 Hz repetition frequency. The maximum energy per pulse was 5.5 mJ. Half of it could be transferred to the cavity for the QE and relaxation time experiments. The maximum available peak power of 0.518 MW at the cathode was two times higher than the power needed for the nominal operation of the gun, when 1 nC bunches are generated within 20 ps. The preliminary relaxation time experiment was performed with the TJNAF cavity, operating at 1.42 GHz. For that experiment the cavity had to be attached to a straight vacuum tube oriented vertically upward, to enable direct irradiation with the laser light via the sapphire window installed at the top-plate of the vertical cryostat. The 3 m long vacuum tube contaminated the cavity with particulates and degraded its performance. At 3 MV/m Q_o was only $2.25 \cdot 10^9$, almost 3 times lower than Q_o measured at this gradient in the RF-performance test. When the Nb wall was irradiated with the maximum available laser power, Q_o dropped to $\sim 1.6 \cdot 10^9$, but the cavity did not quench and behaved still very stable. The additional dissipation, due to the locally broken Cooper pairs in the irradiated area, was 5.2 mW. The surface resistance, r_s , of the irradiated area increased during the laser pulse by a factor of 630. The ratio of r_s after and before the irradiation indicates that the concentration of quasi-particles rose to their equilibrium concentration at 8 K. According to the theoretical model, their relaxation time is shorter than 100 ps at this temperature.

ACKNOWLEDGMENT

We would like to express our gratitude to colleagues at DESY, BNL, INS and TJNAF from whom we received technical support.

REFERENCES

- [1] J. Sekutowicz et al., "Nb-Pb Superconducting RF-gun", TESLA-FEL Report 2005-09, DESY, 2005.
- [2] M. Ferrario, NIM A 472, (2001), 303-308.
- [3] J. Sekutowicz, Proceed. ICFA Workshop on The Physics and Applications of High Brightness Electron Beams, Erice, Italy, 9-14 October, 2005; http://www.physics.ucla.edu/PAHBEB2005/talks/10_oct_2005/index.htm
- [4] A. Michalke et al., Proc. EPAC92, Berlin, Germany, 1992, p. 1014, <http://www.jacow.org>.
- [5] D. Janssen et al., Proc. PAC97, Vancouver, Canada, 1997, p. 28238, <http://www.jacow.org>.
- [6] T. Srinivasan-Rao et al., Proc. PAC03, Portland, Oregon, p. 92, <http://www.jacow.org>.
- [7] J. Sekutowicz et al., "Nb-Pb Superconducting RF-Gun", TESLA-FEL Rep.-2005-09, DESY, 2005.
- [8] J. Smedley et al., Proc. EPAC2004, Lucerne, Switzerland, p. 1126, <http://www.jacow.org>.
- [9] J. Smedley et al., "Photoemission Tests of a Pb/Nb Superconducting Photoinjector", these Proceedings.